Supporting information for

Supramolecular Self-Assembly of Morphology-dependent Luminescent Ag Nanoclusters

Xiaofang Jia, Jing Li and Erkang Wang

State Key Laboratory of Electroanalytical Chemistry, Changchun Institute of Applied Chemistry, Chinese Academy of Sciences, Changchun, Jilin, 130022, and Graduate School of the Chinese Academy of Sciences, Beijing, 100039, China

E-mail: ekwang@ciac.ac.cn

Materials and methods

Materials

D-penicillamine (DPA), L-penicillamine (LPA), and racemic DL-penicillamine (DLPA) were obtained from Alfa Aesar (Tianjin, China). $AgNO_3$ and other reagents were purchased from Beijing Chemical Works (Beijing, China). Water used throughout all experiments was purified with the Millipore system (18.2 MΩ). All glassware was washed with *aqua regia* and rinsed with ultrapure water.

Apparatus and characterization

High-resolution transmission electron microscope (HRTEM) was recorded on JEM-2100F operated at 200 kV. Scanning electron microscopy (SEM) was conducted using an XL30 ESEM FEG scanning electron microscope. X-ray photoelectron spectroscopy (XPS) was investigated by using ESCALAB-MKII 250 photoelectron spectrometer (VG Co.) with Al Kα X-ray radiation (1486.6 eV) for excitation. IR spectra were taken on a VERTEX Fourier transform infrared spectrometer (Bruker). X-ray power diffraction (XRD) pattern was recorded on a D8 Focus diffractometer (Bruker) with a Cu Kα radiation source (λ= 0.15406 nm). Negative-ion electrospray ionization mass spectrometry (ESI MS) measurements were performed on a LTQ linear ion trap mass spectrometer (Thermo, San Jose, CA, USA), equipped with a conventional ESI source. Steady-state Fluorescence spectroscopy was collected with a Fluoromax-4 spectrofluorometer (Horiba Jobin Yvon Inc. France) using 2.5 nm/ 2.5 nm slit widths of excitation and emission. The luminescence decay curves were detected by a Lecroy Wave Runner 6100 Digital Osilloscope (1 GHz) using a tunable laser (pulse width = 4 ns, gate = 50 ns) as the excitation (Contimuum Sunlite OPO). UV-vis absorption spectra were obtained using a Cary 50 Scan UV-visible spectrophotometer (Varian, USA). The quantum yields were measured at room temperature with the absolute quantum yield measurement system C9920-02 (Hamamatsu Photonics K. K., Japan), which comprises an excitation light source, monochromator, an integrating sphere capable of nitrogen gas flow and a CCD spectrometer for detecting the whole spectral range simultaneously.

Synthesis of AgNCs

For AgNCs S3, $AgNO_3$ aqueous solution (0.4 mL, 0.1 M) was added to 9.6 mL DPA (8.33 mM) solution in 250 mL beaker. The mixture was heated in a domestic microwave oven (800W, Galanz) for 3 min. Finally, the obtained product was collected and centrifugated at 8000 rpm for 10 min followed by washing thoroughly with water for three times. Then the product was freeze-dried under the vacuum and stored in the refrigerator (-20 °C) for long-term preservation. For AgNCs S1, $AgNO_3$ aqueous solution (30 μL, 0.1 M) was added to 2.97 mL DPA (2.02 mM) solution in 100 mL beaker. Then the procedure was similar to S3. For DLPA protected AgNCs S2, the procedure was the same to the S3 except the ligand DLPA.

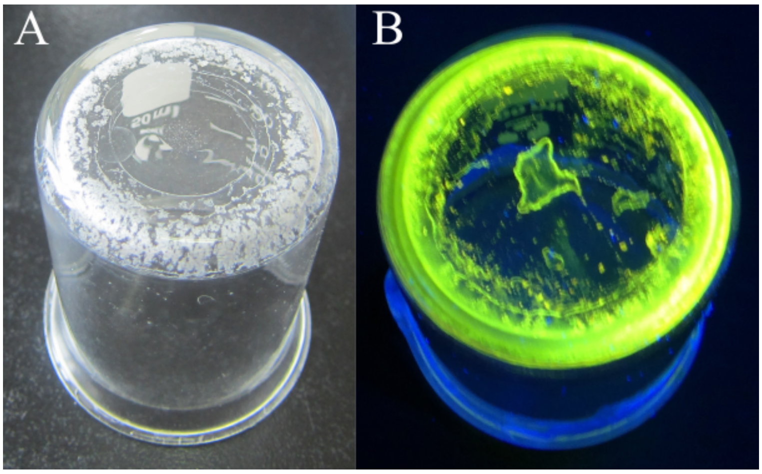

Figure S1. The photographs of the resultant product S1.

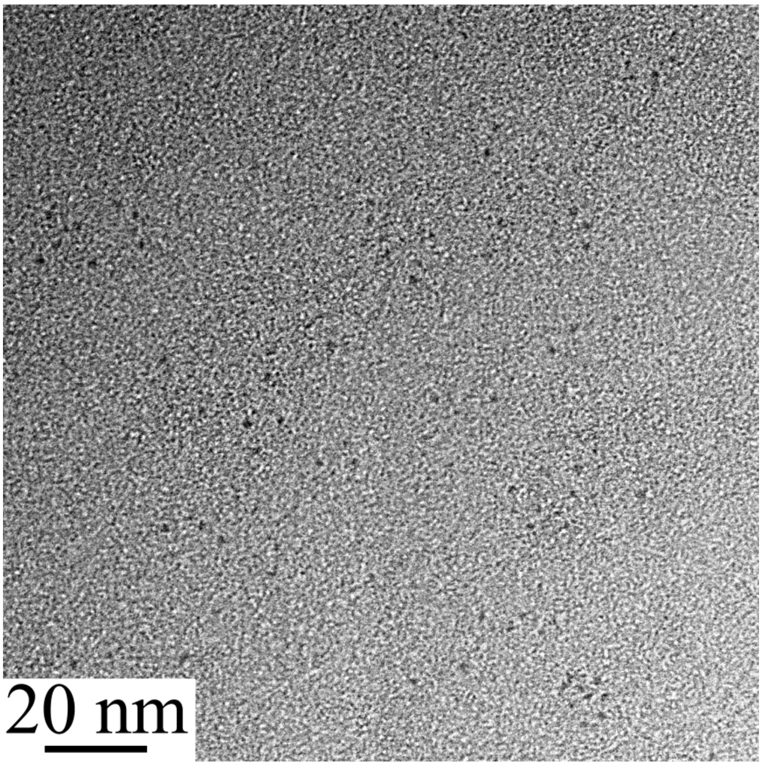

Figure S2. The representative TEM image of the as-prepared AgNCs in dispersed state by addition of NaOH.

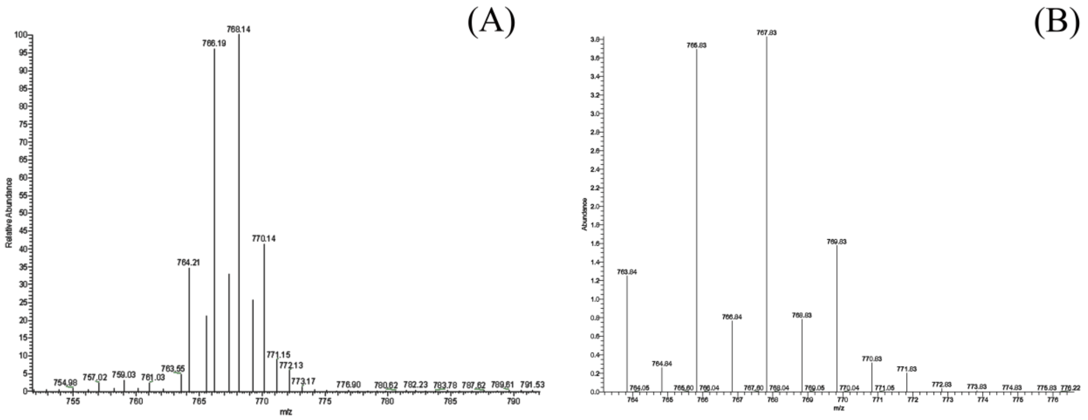

Figure S3. (A) Experimental and (B) simulated isotopic pattern of $[Ag_3L_3]^-$.

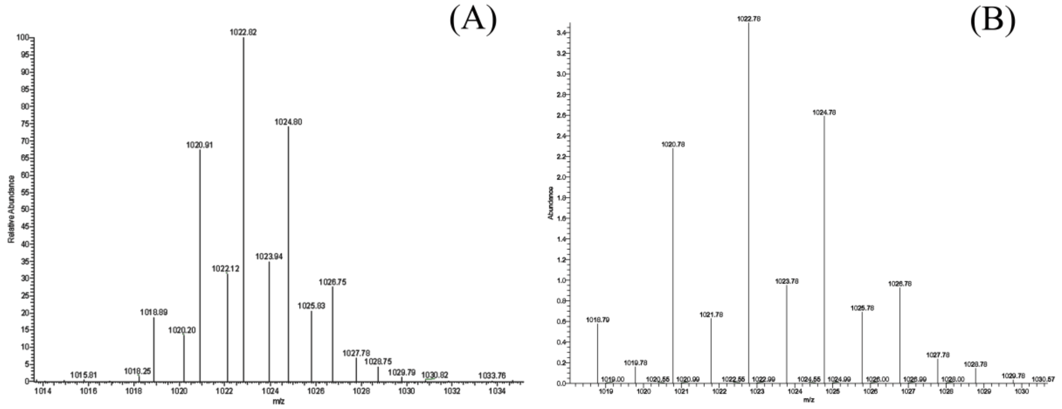

Figure S4. (A) Experimental and (B) simulated isotopic pattern of $[Ag_4L_4]^-$.

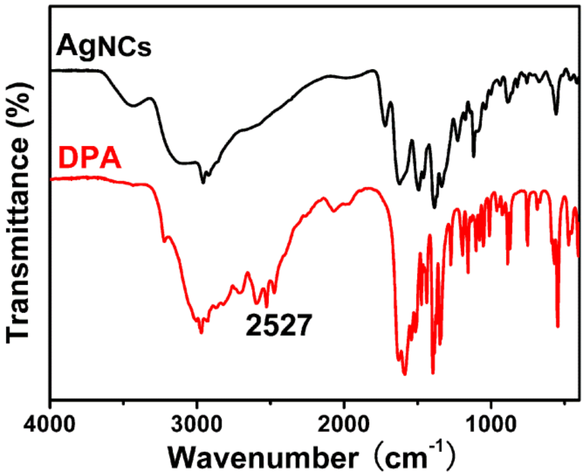

Figure S5. FTIR spectra of pure DPA and DPA-capped AgNCs.

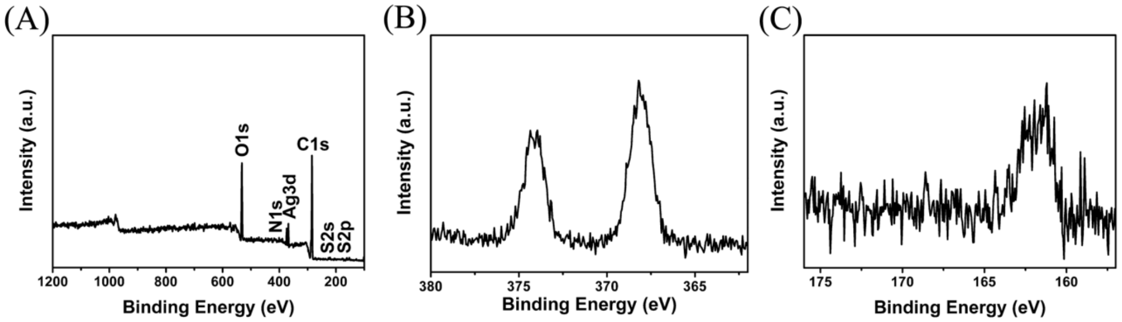

Figure S6. (A)XPS survey spectrum of the AgNCs; (B) XPS of Ag 3d electrons in AgNCs; (C) XPS of S 2p electrons in AgNCs.

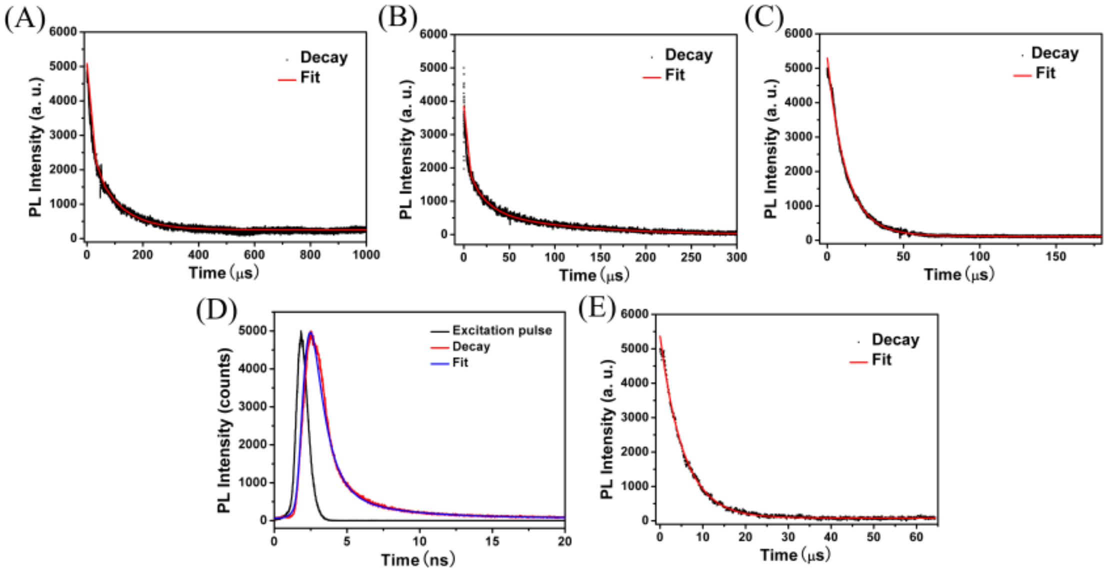

Figure S7. PL decay profile of (A) S1 (λ_{em} = 543 nm), (B) S2 (λ_{em} = 550 nm), and (C) S3 (λ_{em} = 588 nm) at the excitation of 350 nm; PL decay profile of (D) S4 (λ_{em} = 425 nm, λ_{ex} = 377 nm) and (E) S4 (λ_{em} = 588 nm, λ_{ex} = 355 nm). The fitted curves were overlaid on the experimental data.

Table S1. Lifetimes of AgNCs at different emissions.

Sample Name	S1	S2	S3	S4	S4
λ_{em} (nm)	543	550	588	425	588
λ_{ex} (nm)	350	350	350	377	355
τ_1	2.64 μs	14.50 μs	11.90 μs	0.94 ns	5.44 μs
A_1[a]	3.7%	13.4%	89.9%	67.7%	100%
τ_2	19.04 μs	94.67 μs	30.54 μs	4.45 ns	-
A_2	24.5%	86.6%	10.1%	32.3%	-
τ_3	106.7 μs	-	-	-	-
A_3	71.8%	-	-	-	-
τ_{ave}[b]	81.41 μs	83.90 μs	13.78 μs	2.07 ns	5.44 μs

[a] The fractional contribution was calculated according to $A_i = \alpha_i\tau_i/\Sigma\alpha_j\tau_j$, where τ_i and α_i represent the decay time and the amplitudes of the components at $t = 0$, respectively; [b] The average lifetime was calculated according to $\tau_{ave} = \Sigma A_i\tau_i$; [c] The multiexponential decays are related to AgNC heterogeneous aggregated states (Chem. Eur. J., 2013, 19, 4110-4116).

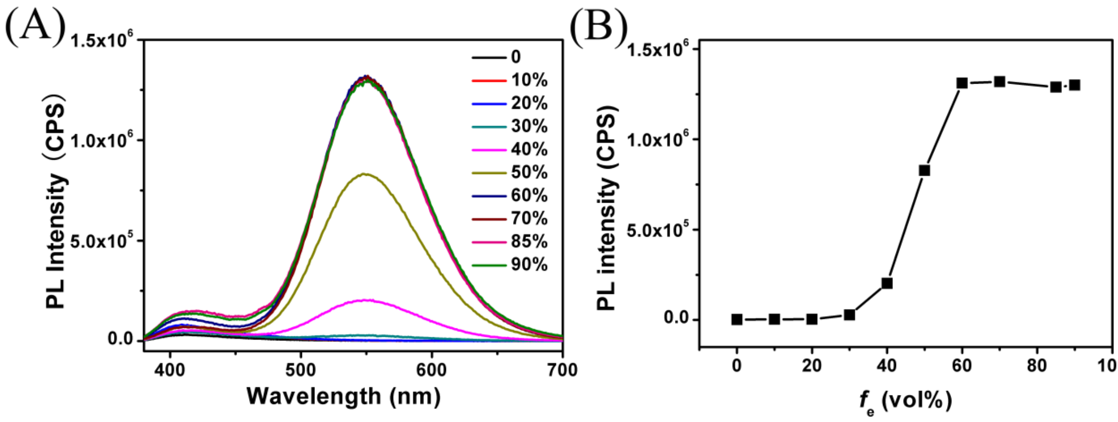

Figure S8. (A) PL spectra of AgNCs S2 in the ethanol/water mixtures with different columetric fractions of ethanol (f_e, vol%); (B) plots of PL intensity of AgNCs S2 versus f_e.

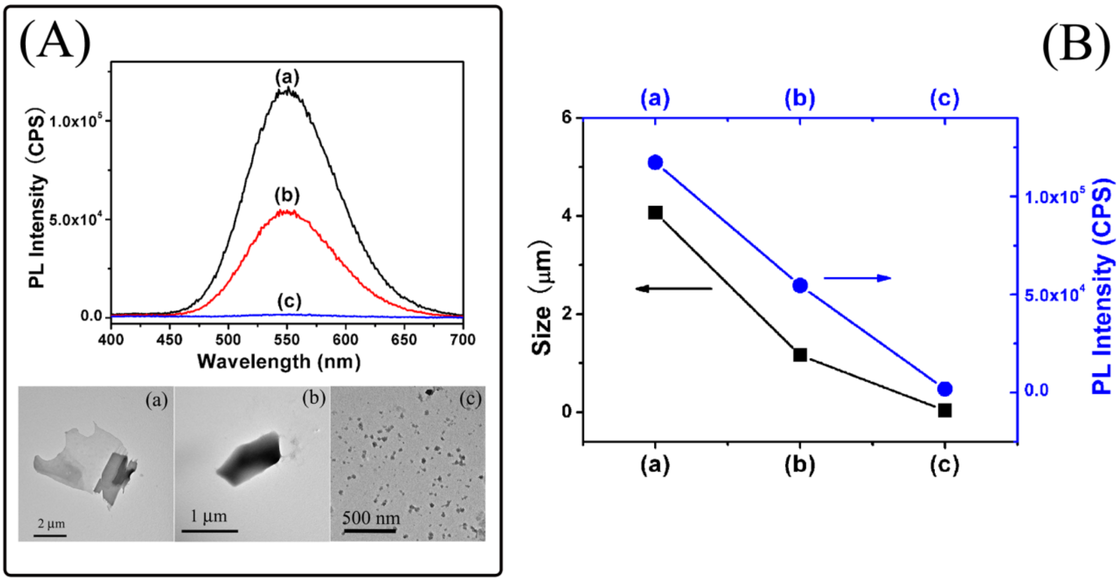

Figure S9. (A) The PL spectra and the corresponding TEM images of AgNC S2 aggregates (sample a, b, c); (B) Plots of size and PL intensity of AgNC S2 aggregates (sample a, b, c).

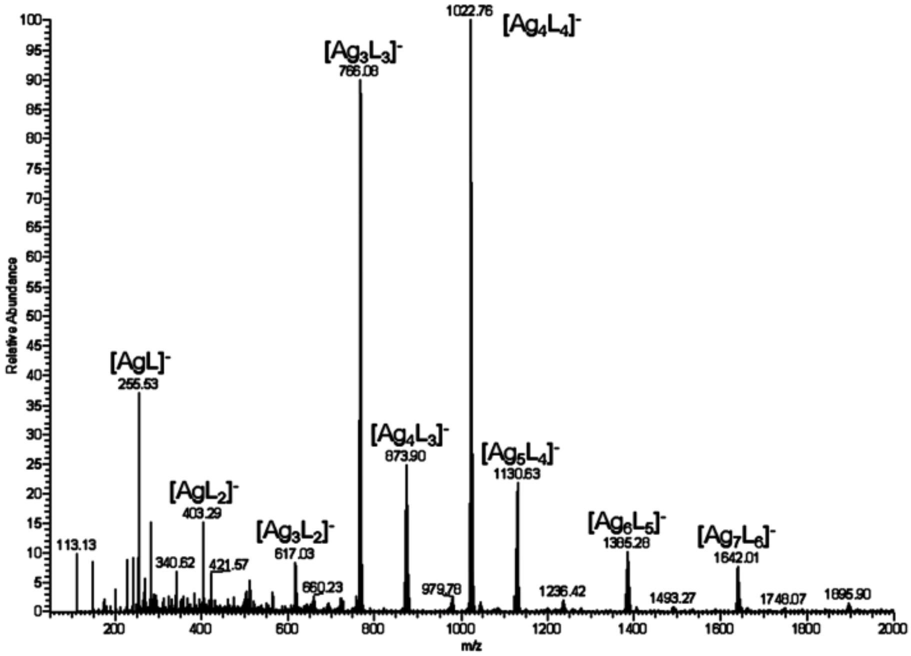

Figure S10. Negative-ion ESI-MS measurement of AgNCs S3 (where L stands for $C_5H_{10}O_2NS$).

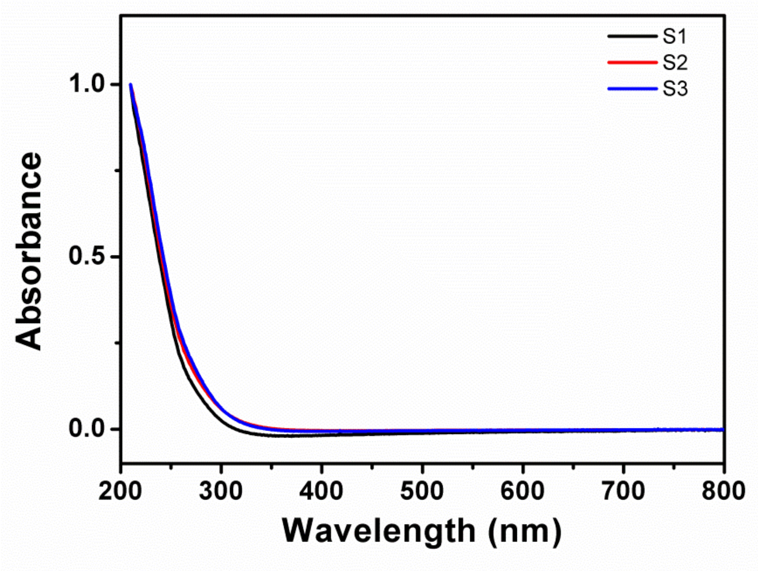

Figure S11. Absorption spectra of AgNCs S1, S2 and S3 aqueous solution.

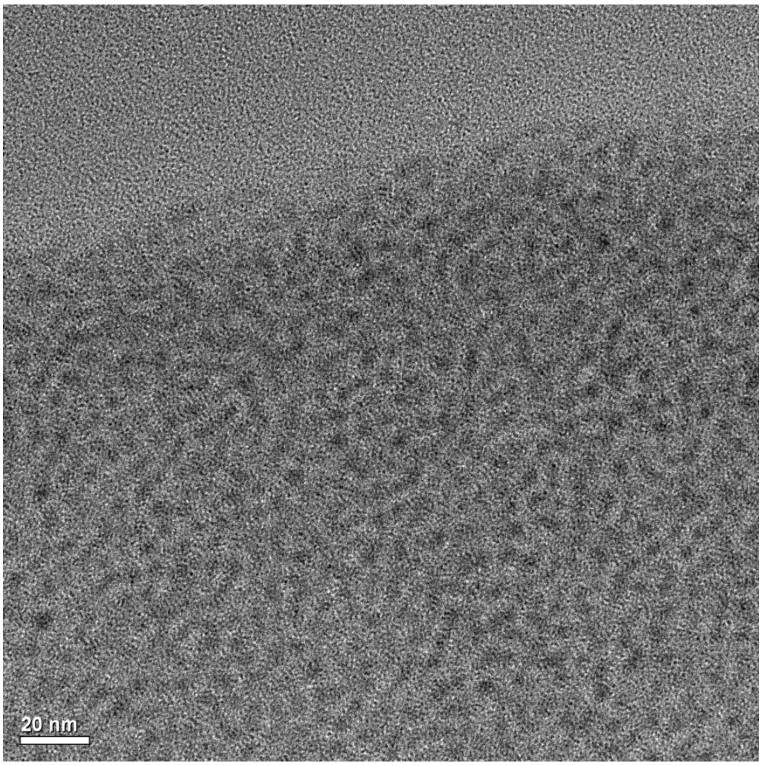

Figure S12. HRTEM image of the flake structure of AgNC S2 aggregates.

Table S2. Observed interlayer (axial) spacing (*kd* values) from (0*k*0) reflections.

	S2		S3	
(0*k*0)	*d* (Å)	Interlayer Spacing *b* = *kd* (Å)	*d* (Å)	Interlayer Spacing *b* = *kd* (Å)
(010)	12.63	12.63	12.22	12.22
(020)	6.34	12.68	6.16	12.32
(030)	-	-	4.11	12.33
(040)	-	-	3.09	12.36
(050)	2.55	12.75	2.45	12.25
(060)	2.12	12.72	-	-
Arithmetic Mean	12.70		12.30	

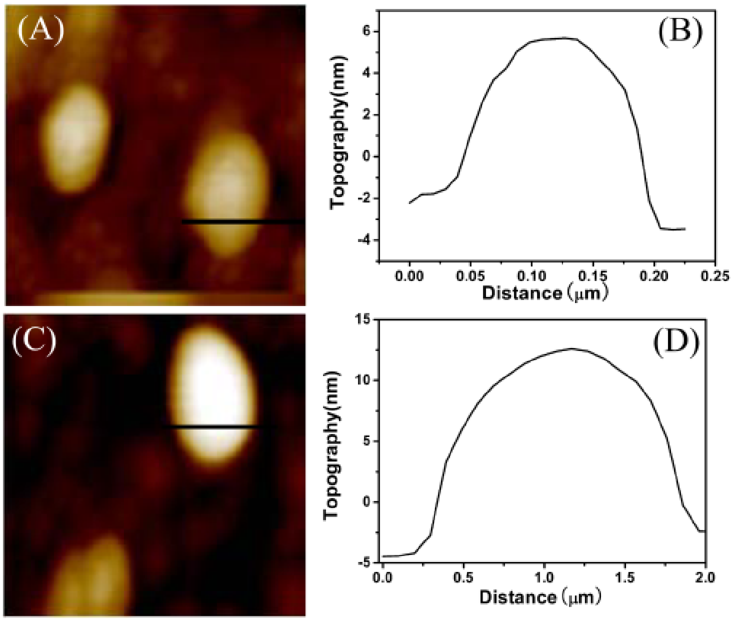

Figure S13. (A) The AFM topography image of AgNCs S1 and (B) the corresponding cross-section line scan profiles; (C) The AFM topography image of AgNCs S2 and (D) the corresponding cross-section line scan profiles. Note: For AFM characterization, the suspension of S1 and S2 was diluted. After dilution, the lamellar structures became thin as comparison with the high concentration sample used in the SEM characterization.